bioRxiv preprint doi: https://doi.org/10.1101/587386; this version posted March 24, 2019. The copyright holder for this preprint (which was not certified by peer review) is the author/funder. All rights reserved. No reuse allowed without permission.

A tissue-like platform for studying engineered quiescent human T-cells' interactions with dendritic cells

Enas Abu-Shah[1,2*], Philippos Demetriou[1], Viveka Mayya[1], Stefan Balint[1], Mikhail A. Kutuzov[2], Omer Dushek[2], Michael L. Dustin[1,3*]

[1]Kennedy Institute of Rheumatology, University of Oxford, Oxford OX3 7FY, UK.
[2]Sir William Dunn School of Pathology, University of Oxford, Oxford OX1 3RE, UK.
[3]Skirball Institute of Biomolecular Medicine, New York University School of Medicine, New York, NY 10016, USA.
*Correspondence: enas.abushah@path.ox.ac.uk, omer.dushek@path.ox.ac.uk, michael.dustin@kennedy.ox.ac.uk

bioRxiv preprint doi: https://doi.org/10.1101/587386; this version posted March 24, 2019. The copyright holder for this preprint (which was not certified by peer review) is the author/funder. All rights reserved. No reuse allowed without permission.

Abstract

Research in the field of human immunology is restricted by the lack of a system that reconstitutes the *in-situ* activation dynamics of quiescent human antigen-specific T-cells interacting with dendritic cells. Here we report a tissue-like system that recapitulates the dynamics of engineered primary human immune cell. Our approach facilitates real-time single cell manipulations, tracking of interactions and functional responses complemented by population-based measurements of cytokines, activation status and proliferation.

Main Text

The field of human immunology has gained much attention in the last few decades with the increasing realisation that despite the tremendous utility of mouse models, they can only provide limited insight for advancing translational research [1,2]. Most of the research in human immunology is based on observational studies, whereby, for example, data sets of gene expression profiles are used to identify disease biomarkers. Although these studies promote our understanding and help in developing hypotheses about disease mechanisms, they fall short, and experimental research is needed [3]. The classical tools in experimental human immunology rely heavily on immortalised cell lines, stimulated clonal lines, peripheral blood, and more rarely humanised mouse models. Each of these tools has its limitation. Cell lines have diverged tremendously from primary cells, making their signalling machinery and response thresholds no longer representative; bulk peripheral blood assays lack the spatial organisation of tissues; and humanised mouse models have only a portion of their system "humanised", rendering the remaining parts confounding factors. To address these limitations, we introduce a holistic approach to allow researchers to manipulate and study human immune cells in a tissue-like environment with minimal aberrations to their natural behaviours. We report a toolkit that achieves two critical goals for engineering T-cells: (1) high efficiency TCR expression and maintenance of T-cell motility, activation dynamics and viability using mRNA electroporation and (2) a tissue-like 3D culture (Scheme).

Successful engineering of T-cells involves the expression of a functional and stable TCR, as well as the preservation of important cellular characteristics. One such characteristic is cell motility which is essential for efficient antigen search. Here, we have optimised the procedures to engineer naïve human CD4 and CD8 T-cells using mRNA electroporation. The common approach to render T-cells antigen specific relies on lentiviral transduction of the TCR

bioRxiv preprint doi: https://doi.org/10.1101/587386; this version posted March 24, 2019. The copyright holder for this preprint (which was not certified by peer review) is the author/funder. All rights reserved. No reuse allowed without permission.

which requires prior expansion of T-cells to achieve high expression efficiency and hinders the study of natural quiescent populations, namely naïve and memory T-cells [4]. To avoid the need for cell expansion, it is possible to use electroporation to deliver the genetic materials. However, reported approaches using electroporation suffer from low efficiency of expression, low viability, and most importantly impaired cell motility (unpublished observations), a critical consideration in the context of delivery to target tissues. Using a square-wave electroporation apparatus, we are able to express the **1G4** TCR, specific to the NY-ESO tumour associated antigen [5] in naïve (Fig. 1a) and memory (Supplementary Fig. 1a) CD8 T-cells as well as the **868** TCR specific for the HIV gag protein [6] (Supplementary Fig. 1b), both presented by HLA-A*0201. Successful pairing of the alpha and beta heterodimer of the TCR is important for the expression and assembly at the cell surface, this was achieved by introducing cysteine modifications in the TCR chains (Supplementary Fig. 1b and Table 1) [7], as well as co-transfection with the human CD3ζ (Supplementary Fig. 1c), as the endogenous protein is most likely sequestered by the endogenous TCR limiting the expression of the introduced TCR. The functionality of naïve CD8 T-cells following TCR electroporation was confirmed by the formation of a mature immunological synapse (IS, Fig.1b), and the upregulation of the activation marker CD69 (Supplementary Fig. 2a). The efficiency of TCR expression varied among donors with a mean value of 81 ± 7% (mean±SD, n=13), with more than 90% cell viability and 80-90% cell recovery.

The induction of expression of an exogenous TCR in CD4 T-cells is considerably harder than in CD8 T-cells [4]. Using natural sequences or the introduction of cysteine modifications used for **1G4** and **868** failed to induce expression of TCRs in naïve CD4 T-cells. However, replacing the constant region of the human TCR with that of mouse TCR (Table 2) [8] allowed for successful chain pairing and we were able to achieve expression in 72 ± 8.9% (mean±SD, n=15) of the cells detected using H57 mAb against the mouse Cβ. We have successful expressed three different HLA-DPB1*04 restricted TCRs in naïve CD4s: **6F9** (Fig.1c) and **R12C9**, both specific to the MAGE-A3 protein [9] and **SG6** specific for NY-ESO [10] (Supplementary Fig. 1d). The expression of **SG6** was consistently lower than **6F9** and **R12C9** in naïve CD4 T-cells. However, when the same TCRs were electroporated into previously activated CD4 T-cells, high expression levels were achieved in 97.8 ± 1% (mean±SD, n=15) of the cells (Supplementary Fig.1e). The functionality of the naïve CD4 T-cells upon TCR electroporation was confirmed by IS formation (Fig. 1d) and T-cell activation (Supplementary Fig. 2b).

bioRxiv preprint doi: https://doi.org/10.1101/587386; this version posted March 24, 2019. The copyright holder for this preprint (which was not certified by peer review) is the author/funder. All rights reserved. No reuse allowed without permission.

Using the square-wave electroporator we were able to maintain the motile behaviour and interaction dynamics of naïve CD8 T-cells expressing **1G4**, at similar levels to those of untouched cells, on 2D stimulatory 'spots' (Supplementary Fig. 3 , Video 1 and [11]).

Naïve T-cells get activated by interacting with professional antigen presenting cells (APCs); the most potent are dendritic cells (DCs). The closest model for *bona fide* DCs is monocyte-derived DCs (moDCs) with well-established protocols for their generation. The caveat with those protocols is their extended duration (7-10 days) [12], a time-frame which may alter autologous T-cells' phenotype. We therefore optimised a 48 h protocol [13] to generate fully matured moDCs. During the first 24 h monocyte differentiation into DC was induced, followed by 24 h maturation to get activated DCs (acDC) (Fig. 1e). The "express" moDCs are able to upregulate MHC and other costimulatory molecules to a similar extent as the "classical" moDC (Supplementary Fig. 4a) and produce a common profile of soluble factors (Supplementary Fig. 4b). We have also quantified peptide loading on these cells and achieved levels similar to those previously reported with other APCs (Supplementary Fig. 4c) [14].

T-cells and DCs interactions have been extensively studied in mice using explants and intravital imaging [15], such studies are practically impossible in humans. Furthermore, accurate control and manipulation of parameters such as antigen dose and cell ratios is limited. Having successfully engineered naïve human T-cells we set out to establish a flexible 3D platform to interrogate their dynamics and interactions with APC using a multitude of correlated functional readouts. The desired platform should: (1) support the culture of T-cells and APCs for multiple days, (2) support the motility of the cells, (3) allow live imaging, (4) enable downstream analysis and (5) be easy to use. To achieve these goals we chose collagen I based 3D matrices[16], which we optimised to support the culture of human immune cells. Culturing cells in the presence of human serum (HS) results in better basal motility than FBS (Fig. 2a, Supplementary Fig. 5a and Video 2), which is significantly enhanced by the addition of homeostatic chemokines such as CCL19 (Supplementary Video 3), CCL21 and CXCL12 (Supplementary Video 4). However, only CXCL12 is able to maintain high motility in cultures with FBS. We have explored different sources of collagen I (bovine, human and non-tryptic collagen) and other complex extracellular matrices, ECM (Supplementary Fig. 5b). All collagens were equally good in supporting motility and interactions, while more advanced ECM may have a marginal advantage for motility. Yet, the larger batch variation, higher background activation and the complexity in extracting cells for downstream analysis weighed against adopting them for our assays. In our view, the use of bovine collagen-I as the 3D

bioRxiv preprint doi: https://doi.org/10.1101/587386; this version posted March 24, 2019. The copyright holder for this preprint (which was not certified by peer review) is the author/funder. All rights reserved. No reuse allowed without permission.

scaffold, with human serum in media, and CXCL12 to enhance motility provides an optimal 3D system.

We present here a proof of concept to the usefulness of our set-up by interrogating naïve CD8 T-cells activation. We used live cell imaging to follow the interactions in real-time by upregulation of CD69 (Fig. 2b and Supplementary Video 5) as well as calcium flux (Supplementary Fig. 6, 7a and Video 6). We observed major changes in interaction dynamics as a function of peptide affinity [17] (Fig. 2c). A high affinity peptide, NY-ESO-9V, (Supplementary Video 7) induced T-cell arrest, whereas a lower affinity peptide, NY-ESO-9L, (Supplementary Video 8), led to similar dynamics as a null peptide (Supplementary Video 9) where no stable contacts are formed. Since our 3D culture offers a relatively simple way to extract cells for flow cytometry and downstream analyses, we were able to correlate the interaction dynamics with the activation state of the cells and observe marginal differences in the response relative to the major differences in dynamics (Fig. 2d). Using our system, we are also able to monitor cytokine production (Supplementary Fig.7 b), proliferation (Supplementary Fig. 7c) and intracellular activation markers (Supplementary Fig. 7d). In order to study the interaction dynamics of T-cells at different time points we can pre-load the acDCs prior or following gel polymerisation to mimic the delivery of antigen to lymph nodes (Supplementary Fig. 7e and Videos 10-11, respectively). Finally, since we are able to engineer both CD4 and CD8 T-cells with unique TCRs we can interrogate the dynamics of CD4 T-cells help to CD8 T-cells [18] (Fig. 2e, Supplementary Video 12) where the activation of CD4 T-cells (Fig.2f, left) coincides with enhanced maturation of the acDCs (Fig. 2f, middle) and enhanced activation of the CD8 T-cells (Fig. 2f, right).

In this report, we present, to the best of our knowledge, a unique and first of its kind holistic approach to engineer quiescent antigen specific human T-cells and study them in a context akin to physiological settings. Our tools are widely applicable to generate T-cells expressing different receptors and other proteins with high efficiency and minimal adverse effects associated with other engineering methods, which are essential for implementation of a successful translational approach. We provide a proof of concept where our system is used to probe the dynamics of T-cell/APC interactions as a function of peptide affinity and recapitulate CD4 help to CD8 T-cells. Our experimental approach can be further extended towards reconstitution of more complex biology such as tumour infiltrating lymphocytes and the role of regulatory T-cells in cancer. We believe that the mechanical and biophysical features introduced by our platform provide greater fidelity to *in vivo* conditions and will improve

bioRxiv preprint doi: https://doi.org/10.1101/587386; this version posted March 24, 2019. The copyright holder for this preprint (which was not certified by peer review) is the author/funder. All rights reserved. No reuse allowed without permission.

predictive power of pre-clinical studies in all human cell-based systems. We propose that our system should be integrated with other classical and computational approaches to enhance translational research.

Methods

Detailed methods are available online

Acknowledgements

We thank Vincenzo Cerundulo for the 1G4 TCR sequence, Andrew Sewell for the 868 TCR plasmid, Steven Rosenberg for the 6F9, R12C9 and SG6 TCR sequences and James Riley for pGEM-64A plasmid. We thank Jehan Afrose for the generation of recombinant proteins. We thank the NIH tetramer facility for providing pMHC monomers. We thank Arbel Artzy-Schnirman for critical reading of the manuscript and help with graphical figures. We thank Kinneret Keren, Erez Braun, Anton van der Merwe, Marion H. Brown and David Depoil for discussions and feedback.

The work has been supported by an UCB-Oxford Post-doctoral Fellowship to E.A-S., European Research Council ERC-2014-AdG_670930 for V.M. and S.B., Kennedy Trust for Rheumatology (KTRR) Prize Studentship to P.D., a Wellcome Trust Principal Research Fellowship 100262Z/12/Z and a grant from KTRR to M.L.D., and a Wellcome Trust Senior Research Fellowship (207537/Z/17/Z) for O.D.

Author contributions

E.A-S. designed and performed the experiments. P.D., V.M. and S.B. contributed to the experiments. M.K. contributed valuable reagents and helped with sequence alignment. E.A-S., O.D. and M.L.D. wrote the manuscript. All authors discussed and approved the manuscript.

References

1 Wagar, L. E., DiFazio, R. M. & Davis, M. M. Advanced model systems and tools for basic and translational human immunology. *Genome medicine* **10**, 73-73, doi:10.1186/s13073-018-0584-8 (2018).

2 Council, M. R. *MRC Strategic Review of Human Immunology*. (2008).

bioRxiv preprint doi: https://doi.org/10.1101/587386; this version posted March 24, 2019. The copyright holder for this preprint (which was not certified by peer review) is the author/funder. All rights reserved. No reuse allowed without permission.

3 Davis, M. M. A prescription for human immunology. *Immunity* **29**, 835-838, doi:10.1016/j.immuni.2008.12.003 (2008).

4 Dai, J. *et al.* Human immunodeficiency virus integrates directly into naive resting CD4+ T cells but enters naive cells less efficiently than memory cells. *Journal of virology* **83**, 4528-4537, doi:10.1128/JVI.01910-08 (2009).

5 Chen, J.-L. *et al.* Identification of NY-ESO-1 peptide analogues capable of improved stimulation of tumor-reactive CTL. *The Journal of Immunology* **165**, 948-955 (2000).

6 Varela-Rohena, A. *et al.* Control of HIV-1 immune escape by CD8 T cells expressing enhanced T-cell receptor. *Nature medicine* **14**, 1390-1395, doi:10.1038/nm.1779 (2008).

7 Cohen, C. J. *et al.* Enhanced antitumor activity of T cells engineered to express T-cell receptors with a second disulfide bond. *Cancer research* **67**, 3898-3903, doi:10.1158/0008-5472.CAN-06-3986 (2007).

8 Cohen, C. J., Zhao, Y., Zheng, Z., Rosenberg, S. A. & Morgan, R. A. Enhanced antitumor activity of murine-human hybrid T-cell receptor (TCR) in human lymphocytes is associated with improved pairing and TCR/CD3 stability. *Cancer research* **66**, 8878-8886, doi:10.1158/0008-5472.CAN-06-1450 (2006).

9 Yao, X. *et al.* Isolation and Characterization of an HLA-DPB1*04: 01-restricted MAGE-A3 T-Cell Receptor for Cancer Immunotherapy. *Journal of immunotherapy (Hagerstown, Md. : 1997)* **39**, 191-201, doi:10.1097/CJI.0000000000000123 (2016).

10 Zhao, Y., Zheng, Z., Khong, H. T., Rosenberg, S. A. & Morgan, R. A. Transduction of an HLA-DP4-restricted NY-ESO-1-specific TCR into primary human CD4+ lymphocytes. *Journal of immunotherapy (Hagerstown, Md. : 1997)* **29**, 398-406, doi:10.1097/01.cji.0000203082.20365.7f (2006).

11 Mayya, V. *et al.* Durable interactions of T cells with T cell receptor stimuli in the absence of a stable immunological synapse. *Cell reports* **22**, 340-349 (2018).

12 Zhou, L. J. & Tedder, T. F. Human blood dendritic cells selectively express CD83, a member of the immunoglobulin superfamily. *The Journal of Immunology* **154**, 3821-3835 (1995).

13 Obermaier, B. *et al.* Development of a new protocol for 2-day generation of mature dendritic cells from human monocytes. *Biological procedures online* **5**, 197-203, doi:10.1251/bpo62 (2003).

14 Walden, P., Zehn, D., Cohen, C. J. & Reiter, Y. Efficiency of peptide presentation by dendritic cells compared with other cell types: implications for cross-priming. *International Immunology* **18**, 1647-1654, doi:10.1093/intimm/dxl098 (2006).

15 Miller, M. J., Wei, S. H., Parker, I. & Cahalan, M. D. Two-Photon Imaging of Lymphocyte Motility and Antigen Response in Intact Lymph Node. *Science* **296**, 1869-1873, doi:10.1126/science.1070051 (2002).

16 Gunzer, M. *et al.* Antigen Presentation in Extracellular Matrix: Interactions of T Cells with Dendritic Cells Are Dynamic, Short Lived, and Sequential. *Immunity* **13**, 323-332 (2000).

17 Aleksic, M. *et al.* Dependence of T cell antigen recognition on T cell receptor-peptide MHC confinement time. *Immunity* **32**, 163-174, doi:10.1016/j.immuni.2009.11.013 (2010).

18 Castellino, F. *et al.* Chemokines enhance immunity by guiding naive CD8+ T cells to sites of CD4+ T cell–dendritic cell interaction. *Nature* **440**, 890, doi:10.1038/nature04651

bioRxiv preprint doi: https://doi.org/10.1101/587386; this version posted March 24, 2019. The copyright holder for this preprint (which was not certified by peer review) is the author/funder. All rights reserved. No reuse allowed without permission.

https://www.nature.com/articles/nature04651#supplementary-information (2006).

19 Zhao, Y. *et al.* High-efficiency transfection of primary human and mouse T lymphocytes using RNA electroporation. *Molecular therapy* **13**, 151-159 (2006).

20 Dustin, M. L., Starr, T., Varma, R. & Thomas, V. K. Supported Planar Bilayers for Study of the Immunological Synapse. *Current Protocols in Immunology* **76**, 18.13.11-18.13.35, doi:doi:10.1002/0471142735.im1813s76 (2007).

21 Mayya, V., Neiswanger, W., Medina, R., Wiggins, C. H. & Dustin, M. L. Integrative analysis of T cell motility from multi-channel microscopy data using TIAM. *Journal of immunological methods* **416**, 84-93 (2015).

22 Mayya, V. *et al.* Synapse propensity of human memory CD8 T cells confers competitive advantage over naïve counterparts. *bioRxiv*, 507392, doi:10.1101/507392 (2018).

Online detailed methods

Reagents

RPMI 1640 (31870074), was purchased from ThermoFisher Scientific. Hyclone Fetal bovine serum was obtained from Fisher Scientific. The following anti-human antibodies were purchased from Biolegend, CD62L (DREG-56), CD3 (OKT3), CD8 (HIT8a), HLA-A2 (BB7.2), CD80 (2D10), CD86 (IT2.2), CD40 (5C3), CD69 (FN50), 4-1BB (4B4-1), CD107 (H4A3), TNFα (Mab11), and anti-mouse TCRβ (H57-97). The following anti-human antibodies were purchased from BD Bioscience, CD45RA (HI100), CD4 (RPA-T4), and CD11c (B-ly6), CD14 (MΦP9). The following anti-human antibodies were purchased from eBioscience CD83 (HB15e) and IFNγ (4S.B3). HLA-A*0201 with 9V was generated and folded in house. HLA-DPB1*04:01 biotinylated monomers were obtained from the NIH tetramer facility. NY-ESO-9V$_{157-165}$ (SLLMWITQV), NY-ESO-4D$_{157-165}$ (SLLDWITQV), NY-ESO-6T$_{157-165}$ (SLLMWTTQV) and NY-ESO-9L$_{157-165}$ (SLLMWITQL), MAGE-A3$_{243-258}$ (KKLLTQHFVQENYLEY), NY-ESO$_{161-180}$ (WITQCFLPVFLAQPPSGQRA), HIV p17 GAG$_{77-85}$ (SLYNTVATL) were purchased from GeneScript with > 95% purity and resuspended in DMF at 1mg/ml and stored at -20^{o}C.

Plasmids and constructs

The sequences for the 1G4 TCR were provided by Vincenzo Cerundolo, the 868 TCR was provided by Andrew Sewell, and all the MHC-II restricted TCRs (SG6, R12C9 and 6F9) were shared by Steven Rosenberg.

All TCRs were synthesised using GeneArt services from ThermoFisher, by adding Kozak sequence and codon optimisation for human expression. The 1G4 and 868 were to include a cysteine modification in the alpha and beta chains (see Supplementary table for sequences).

The MHC-II restricted TCRs were synthesised so that the human constant region was replaced with the mouse constant regions (see Supplementary table for sequences).

bioRxiv preprint doi: https://doi.org/10.1101/587386; this version posted March 24, 2019. The copyright holder for this preprint (which was not certified by peer review) is the author/funder. All rights reserved. No reuse allowed without permission.

The alpha and beta chains were cloned separately into a pGEM-GFP-64A plasmid (gift of James Riley) between HindIII and NotI for MHC-I restricted TCRs and for human CD3ζ and between AgeI and NotI for MHC-II restricted TCRs.

T-cell purification

T-cell were isolated from anonymised leukopoiesis products obtained from the NHS at Oxford University Hospitals by (REC 11/H0711/7). Resting human T-cell subsets were isolated using negative selection kits (Stemcell Technologies), total CD4 or CD8 T-cells were enriched using RosetteSep kits from Stemcell Technologies, followed by EasySep kits for the corresponding naïve and memory sub-population, following the manufacturer's protocol. Cell purity was assayed with anti-CD4, anti-CD8, anti-CD62L and anti-CD45RA and all cells used had >95% purity.

Human CD4 and CD8 T-cells were cultured at 37ºC, 5% CO_2, in RPMI 1640 (Roswell Park Memorial Institute) medium Supplemented with 10% FBS (Gibco), 5% Penicillin-Streptomycin, Penstrep (Gibco), 1x MEM Non-Essential Amino Acids Solution, 20 mM HEPES, 1 mM Sodium Pyruvate, 2 mM Glutamax and 50 μM 2-mercaptoethanol (Sigma) (all from Thermo Fisher unless stated otherwise).

Express monocyte-derived dendritic cell generation

Monocytes were enriched from the same leukopoiesis products as T-cells using RosetteSep kits (Stemcell Technologies), and were then cultured at 1-2x10^6/ml in 12 well-plates with differentiation media containing 50 ng/ml Interleukin 4 (IL-4, 200-04 A, Peprotech) and 100 ng/ml granulocyte-monocyte colony stimulating factor (GM-CSF, 11343125, Immunotools) for 24 h. For maturation the following cytokines were added for an additional 24 h, 1 μM Prostaglandin E_2 (PGE_2, P6532, Sigma), 10 ng/ml Interleukin 1 beta (IL1β, 201-LB-025/CF, Biotechne), 50 ng/ml Tumour Necrosis Factor alpha (TNFα, 300-01A, Peprotech), and 20 ng/ml Interferon gamma (IFNγ ,285-IF-100/CF, Bio-techne). Cell purity of the monocyte population was assessed using antibodies against CD14 and CD11c and typically was above 80%. Any non-monocyte contaminants can be removed by adhering the cells for 2-3 hours immediately following isolation followed by washing any unbound cells and applying the differentiation media.

Peptide loading on DC was quantified using an AlexaFluor 647 conjugated high affinity soluble TCR (c113 against NY-ESO) with a known dye ratio and Quantum MESF AlexaFluor 647 beads as calibration (647, Bangs Laboratories).

Secretion of soluble factors was assessed using 0.5 ml of culture medium, and the corresponding controls of media containing the differentiation and activation cytokines, following the manufacturer's protocol (Proteom Profiler Human XL Cytokine Array kit, ARY022B, R&D Systems).

HLA typing of donors

bioRxiv preprint doi: https://doi.org/10.1101/587386; this version posted March 24, 2019. The copyright holder for this preprint (which was not certified by peer review) is the author/funder. All rights reserved. No reuse allowed without permission.

For antigen specific experiments the donors were assessed for the relevant HLA, for CD8 based experiments 50 µl of whole blood was taken for flow cytometry analysis using an anti HLA-A2 mAb (Clone BB7.2). For CD4 based experiments 50 µl of blood was used to extract DNA using QIAamp DNA Mini kit (51304, Qiagen). The product was used for PCR analysis using the AllSet+ Gold HLA DPB1 high resolution Kit (54070D, vhbio) to determine if expressing the suitable haplotype. We were also able to induce the expression of a single chain dimer of HLA-A*02 in moDCs from donors which were HLA-A*02 negative using the mRNA electroporation approach.

Engineering antigen specific T-cells

To express TCR constructs within resting naïve and memory T-cells, we used mRNA electroporation. mRNA preparations of the relevant TCRα, TCRβ and CD3ζ chains from a linearised pGEM-64A vector or a T7 containing PCR product was done using mMESSAGE mMACHINE T7 ULTRA Transcription kit as per manufacturer's protocol (ThermoFisher, AM1345). The mRNA was purified using MegaClear kit (ThermoFisher, AM1908) and was aliquoted and kept at -80ºC [19]. To achieve high efficiency of expression, mRNA quality was assessed using agarose gels and samples showing any sign of degradation were discarded. Any mRNA preparation with yields bellow 40 µg mRNA per 1 µg of DNA was considered of low quality, finally all mRNA aliquots were stored at concentrations > 1 µg/µl, which can be achieved by concentrating the mRNA product using ammonium acetate precipitation or by combining >3 reactions of *in vitro* transcription during the MegaClear clean-up step.
T-cells were harvested and washed three times with Opti-MEM (LifeTechnologies). The cells were resuspended at 25x10^6/ml and 2.5-5x10^6 cells were mixed with the desired mRNA products and aliquoted into 100-200 µl per electroporation cuvette (Cuvette Plus, 2 mm gap, BTX). For each 10^6 cells CD8 T-cells 5 µg of each TCRα, TCRβ and CD3ζ RNA was used. For 10^6 CD4 T-cells 10 µg of TCRα and TCRβ was used. Cells were electroporated at 300V, 2ms in an ECM 830 Square Wave Electroporation System (BTX). The cells were then collected from the cuvette and cultured in 1 ml pre-warmed media. Amaxa and Neon electroporation systems were also tested but failed in either achieving efficient TCR expression or the affected T-cell motility. In addition, extended culture (>5 days) prior to electroporation also results in marginal reduction in TCR expression efficiency, although not observed for control GFP.
The exogenous TCR can be detected up to 96 h post electroporation.

Supported lipid bilayers (SLB)

SLBs were prepared as previously described [20]. In brief, piranha and plasma cleaned coverslips were mounted on sticky-Slide VI0.4 chamber (ibidi). Small unilamellar liposomes (LUVs) were prepared using 4 mM 18:1 DGS-NTA(Ni), "NTA-lipids", (790404C-AVL, Avanti Polar Lipids,), 4 mM CapBio 18:1 Biotinyl Cap PE (870282C-AVL, Avanti Polar Lipids), "CapBio-lipids", and 4 mM 18:1 (Δ9-Cis) PC, "DOPC-lipids", (850375C-AVL, Avanti Polar Lipids,). NTA-lipids were used at a final concentration of 2 mM and CapBio lipids were used at a

bioRxiv preprint doi: https://doi.org/10.1101/587386; this version posted March 24, 2019. The copyright holder for this preprint (which was not certified by peer review) is the author/funder. All rights reserved. No reuse allowed without permission.

dilution resulting in site density of 30 molecules/μm^2. SLBs were allowed to form by incubating the coverslips with the appropriate LUVs for 20 min at room temperature (RT) followed by a wash with HEPES buffered saline (HBS) Supplemented with 1 mM $CaCl_2$ and 2 mM $MgCl_2$, and human serum albumin (HBS/HSA). The SLBs were loaded with saturating amounts of AlexaFluor568 labelled streptavidin, 5 µg/ml, (S11226, ThermoFisher) for 10 min at RT followed by pMHC at 30 molecules/μm^2 and ICAM-1 200 molecules/μm^2 for 20 min at RT.

Micro-contact printed chambers

Micro-patterned surfaces presenting pMHC molecules were prepared using micro-contact printing by modifying the procedures described previously [11]. Topological masters with repetitive circle patterns of 10 µm in diameter, spaced 30 µm centre-to-centre on a square grid were used to cover the entire channel of sticky-Slide $VI^{0.4}$ chamber (ibidi). The master was used for casting of polydimethylsiloxane (PDMS) elastomer stamps. Sylgard 184 (Dow Corning) was used by mixing 1/7 (v/v) of curing agent to the elastomer. Rectangular stamps of PDMS were coated with biotinylated, AlexaFluor 674 labelled, Fc IgG (AG714, Merck Millipore) at 2 µg/ml in 150 µl of PBS for one hour. The blocks were then rinsed extensively in PBS, PBS with 0.05% Tween-20 and finally in MilliQ-grade water followed by gentle drying with N_2 to remove droplets of water. Fc coated PDMS blocks were stamped onto the cleaned coverslips for 5 minutes under ~20 g of load for efficient transfer. Attempts to directly stamp pMHC, avidin or streptavidin resulted in partially or completely non-functional proteins. Streptavidin stamps were also non-uniform and eroded with subsequent washes. The patterned coverslip was then affixed to the sticky-Slide $VI^{0.4}$ and washed sequentially with MilliQ-grade water and PBS, then coated with 13.5 µg/ml of CCL21 in 30 µl for one hour, followed by 3 µg/ml of ICAM1 in 180 µl for 3 h at 37°C. Coverslips were then used immediately for the following steps or kept with PBS at 4°C overnight. The stamped and protein coated channels were blocked with 10% dialysed FCS (to remove any free biotin) for 30 min at RT. Then unlabelled streptavidin was introduced into the channel at 2 µg/ml for 10 min at RT, washed and followed by 9V/A2 pMHC at 1 µg/ml for 20 min at RT.

Collagen gel chamber assembly

DC were loaded with the mentioned peptide for 90 min at 37°C. For imaging experiments T-cells were labelled with a volumetric dye as described below (*Imaging*) or loaded with cell trace violet (C34557, ThermoFisher) for proliferation assays or otherwise kept unlabelled.

Collagen mix was made by modifying the approach of Gunzer et al [16] using 5 µl 7.5% sodium bicarbonate, 10 µl 10x MEM, 75 µl 3 mg/ml Bovine Collagen I (PureCol) and a chemokine, 1 µg/ml of CCL21 (300-35-100, Peprotech) or CCL19 (300-29B, Peprotech) or 0.3 µg/ml of SDF1-a/CXCL12 (300-28A, Peprotech). All the work with collagen was done on ice to prevent polymerisation. Other matrices tested: VitroCol Human Collagen I (5007-A, CellSystems), Matrigel (at final conc. of ~4 mg/ml, two batches tested with similar results), and GelTrex (A1413301, ThermoFisher, at final concentration of ~8 mg/ml, two batches tested with similar results). All 3D cultures were made with Bovine Collagen I, except for the comparison shown in Supplementary Fig. 5, and mainly with CXCL12 unless otherwise stated.

bioRxiv preprint doi: https://doi.org/10.1101/587386; this version posted March 24, 2019. The copyright holder for this preprint (which was not certified by peer review) is the author/funder. All rights reserved. No reuse allowed without permission.

Cell containing media (15 µl) supplemented with 10% Human serum (S-101B-FR, APS) (or 10% FBS) is added to 35 µl of the collagen mix so that the final culture contained 200,000 CD8, 200,000 CD4s T-cells and DC at varying ratios (typically 1:1, 1:5 and 1:10 to T-cells). Lower cell numbers can be used for functional experiment but the reported numbers here are ideal for good density for imaging.

30µl of the collagen is then added to a µ-slide angiogenesis chamber or sticky-Slide VI$^{0.4}$ chamber (ibidi) and put upside down in a 37ºC incubator with 5% CO_2 for ~60 min (to entrap the cells in the gel as it polymerises). The wells are then topped up with 30 µl media containing the same concentration of chemokines as the gel (for µ-slide angiogenesis) or 100 µl per well (for sticky-Slide VI$^{0.4}$) . For in gel loading experiments, the media contained a peptide at 2x the reported concentration. Samples are either taken for imaging or kept in the incubator for functional analysis.

Extended culture in the 3D system leads to ~50% reduction in cell speed due to chemokine desensitisation and can be overcome by the addition of fresh chemokine after 18 h.

Flow cytometry

1G4 TCR expression was assessed using 9V-HLA-A2 tetramers, **868** TCR expression was assessed using SL9-HLA-A2 streptamers (6-7004-001, iba) and **6F9**, **SG6** and **R12C9** expression was assessed with anti-mouse TCR β (H57) antibody. The MHC II restricted TCRs seem to have very low affinity towards their antigen preventing detection using tetramers (attempts to measure affinity using SPR suggest a Kd bellow 500 µM). In brief, 50,000 cells were stained with 2.5 µg/ml tetramer (9V/A2) or 5 µg/ml streptamers (SL9/A2) or 1 µg/ml antibody for 20 min at 4ºC, washed with PBS containing 2% FBS and 2 mM EDTA and taken for analysis on a flow cytometry machine (FORTESSA X-20, BD).

To analyse samples from collagen gels, the gels were first digested into solution using collagenase VII (Sigma #C0773) at 100 U/ml for 1 h at 37ºC. The supernatant subsequently removed, and the cells stained with the desired antibody combination for 20 min 4ºC. For intracellular staining, the cells were cultured in collagen gels and Brefeldin A or monensin were added after 20 h for 2 h along with a stimulation of Phorbol 12-myristate 13-acetate (PMA, P8139, Sigma) at 1 µg/ml and ionomycin (I0634, Sigma) at 1 µM, the cells were then stained using the FoxP3 intracellular staining kit (00-5523-00, eBioscience) and the desired antibodies. For experiments measuring LAMP1 expression, an antibody against it was added at the start of the culture.

Imaging

Cells are labelled with either one of the volumetric dyes, CMFDA (250 nM, ThermoFisher), CMRA (500 nM, ThermoFisher) or Deep Red (100 nM, ThermoFisher) for 20 min in complete media. For imaging CD69 activation the collagen mixture described above was supplemented with a BV421nlabelled anti-CD69 at 1 µg/ml (adjustments in volume are made to the media to maintain the same final collagen concentration). For calcium imaging T-cells were loaded with 1 µM of Fluo4-AM (ThermoFisher) for 20 min at 37ºC. Cells were imaged using either a Dragonfly Spinning Disk system, a Perkin Elmer Spinning disk or an Olympus FluoView FV1200 confocal microscope using a 30x Super Apochromat silicone oil immersion objective with 1.05 NA. All

bioRxiv preprint doi: https://doi.org/10.1101/587386; this version posted March 24, 2019. The copyright holder for this preprint (which was not certified by peer review) is the author/funder. All rights reserved. No reuse allowed without permission.

microscopes included an environmental chamber to maintain temperature at 37ºC and CO_2 at 5%. Time-lapse images were acquired every 30 or 60s. *z*-scans were acquired every 3 μm.

SLB imaging was performed on an Olympus IX83 inverted microscope equipped with a TIRF module and Photomertrics Evolve delta EMCCD camera using an Olympus UApON 150x TIRF N.A 1.45 objective.

Data analysis

Microscopy data from collagen gels was rendered and analysed using IMARIS software (Bitplane) using built-in analysis tools. Synapse images were analysed using Fiji. Image analysis for micro-contact printing data was done using TIAM [21] as described in [11]. In brief, cells were tracked using DIC images. IRM and fluorescence signal-positive segments of the tracks were used to calculate the attachment rate and the number of cells interacting with stimulatory spots to extract the half-life of interactions where a simple first order rate was used $dA/dt=-k[A]$; where A is cell number and k is the off-rate constant representing the exit from the spots by dissolution of the IS. Data from IMARIS and FlowJo was plotted and analysed in Prism (GraphPad), where all statistical tests were performed.

bioRxiv preprint doi: https://doi.org/10.1101/587386; this version posted March 24, 2019. The copyright holder for this preprint (which was not certified by peer review) is the author/funder. All rights reserved. No reuse allowed without permission.

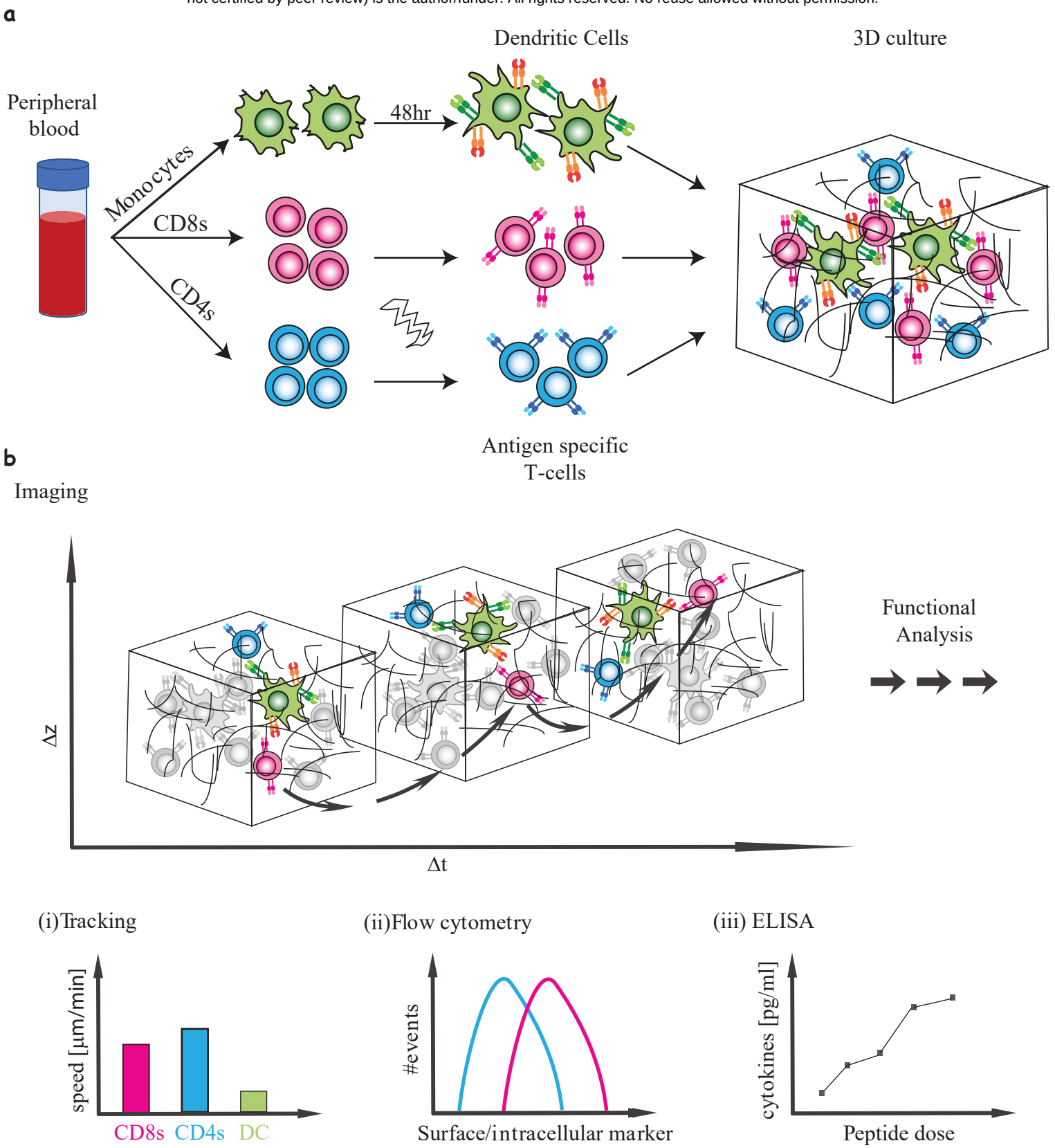

Scheme Abu-Shah et al

bioRxiv preprint doi: https://doi.org/10.1101/587386; this version posted March 24, 2019. The copyright holder for this preprint (which was not certified by peer review) is the author/funder. All rights reserved. No reuse allowed without permission.

Scheme. (a) Isolation of CD4 T-cells, CD8 T-cells and monocytes from peripheral blood. Subpopulations of T-cells can be further isolated and TCR expression is induced by mRNA electroporation. Monocytes are induced to differentiate into DCs, which are also activated with a 48 h express protocol. The cells are then moved into collagen gel-based 3D culture. (b) Cells can be taken for imaging or downstream functional analyses. (i) The imaging can be used to analyse interactions dynamics such as speed or conjugate formation, (ii) Cells can be extracted for flow cytometry, (iii) Cytokine production into the culture can be measured.

bioRxiv preprint doi: https://doi.org/10.1101/587386; this version posted March 24, 2019. The copyright holder for this preprint (which was not certified by peer review) is the author/funder. All rights reserved. No reuse allowed without permission.

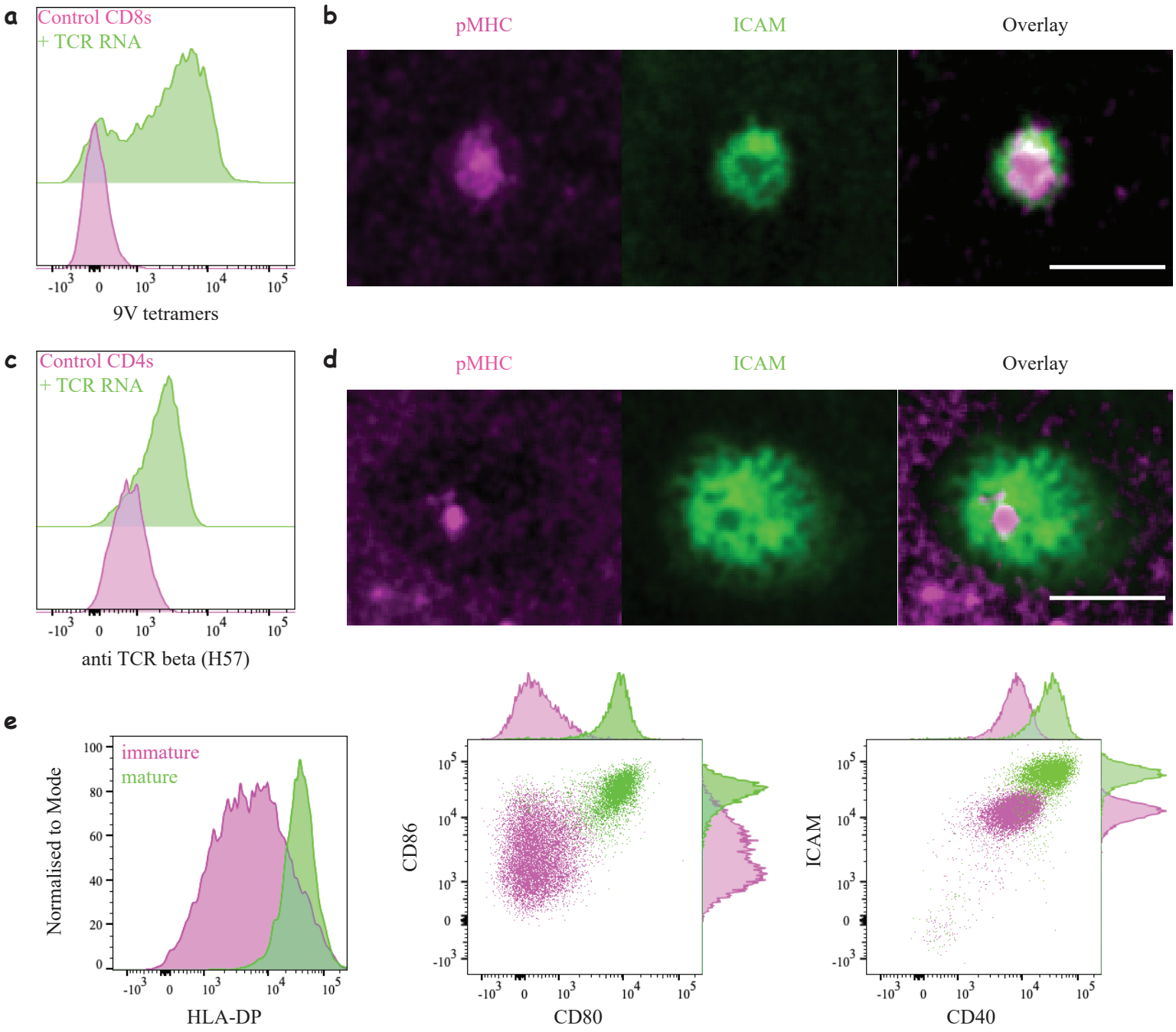

Fig. 1 Abu-Shah et al

bioRxiv preprint doi: https://doi.org/10.1101/587386; this version posted March 24, 2019. The copyright holder for this preprint (which was not certified by peer review) is the author/funder. All rights reserved. No reuse allowed without permission.

Fig.1. Engineering Immune Cells for Antigen-specific Interactions. (a) Expression of **1G4** TCR in naïve CD8 T-cells upon mRNA electroporation using NY-ESO-9V/HLA-A2 tetramer (Representative of N=13). (b) Formation of an immunological synapse by **1G4** expressing naïve CD8 T-cells on supported lipid bilayers (SLBs) with cSMAC enriched with 9V/A2 pMHC (magenta) surrounded by LFA/ICAM1 ring (green). Representative of at least 3 independent repeats. (c) Expression of **6F9** TCR in naïve CD4 T-cells detected using an antibody against the constant region of mouse TCRβ (Representative of N=15). (d) Formation of immunological synapse by **6F9** expressing naïve CD4 T-cells on SLB containing MAGE/DP4 pMHC (magenta). Representative of at least 3 independent repeats. (e) Activation and differentiation profile of "express" monocyte-derived dendritic cells: mature cells (green) upregulate their antigen presentation and costimulatory molecules compared to immature cells (magenta). Representative of at least 3 independent repeats. Scale bars = 5 μm.

bioRxiv preprint doi: https://doi.org/10.1101/587386; this version posted March 24, 2019. The copyright holder for this preprint (which was not certified by peer review) is the author/funder. All rights reserved. No reuse allowed without permission.

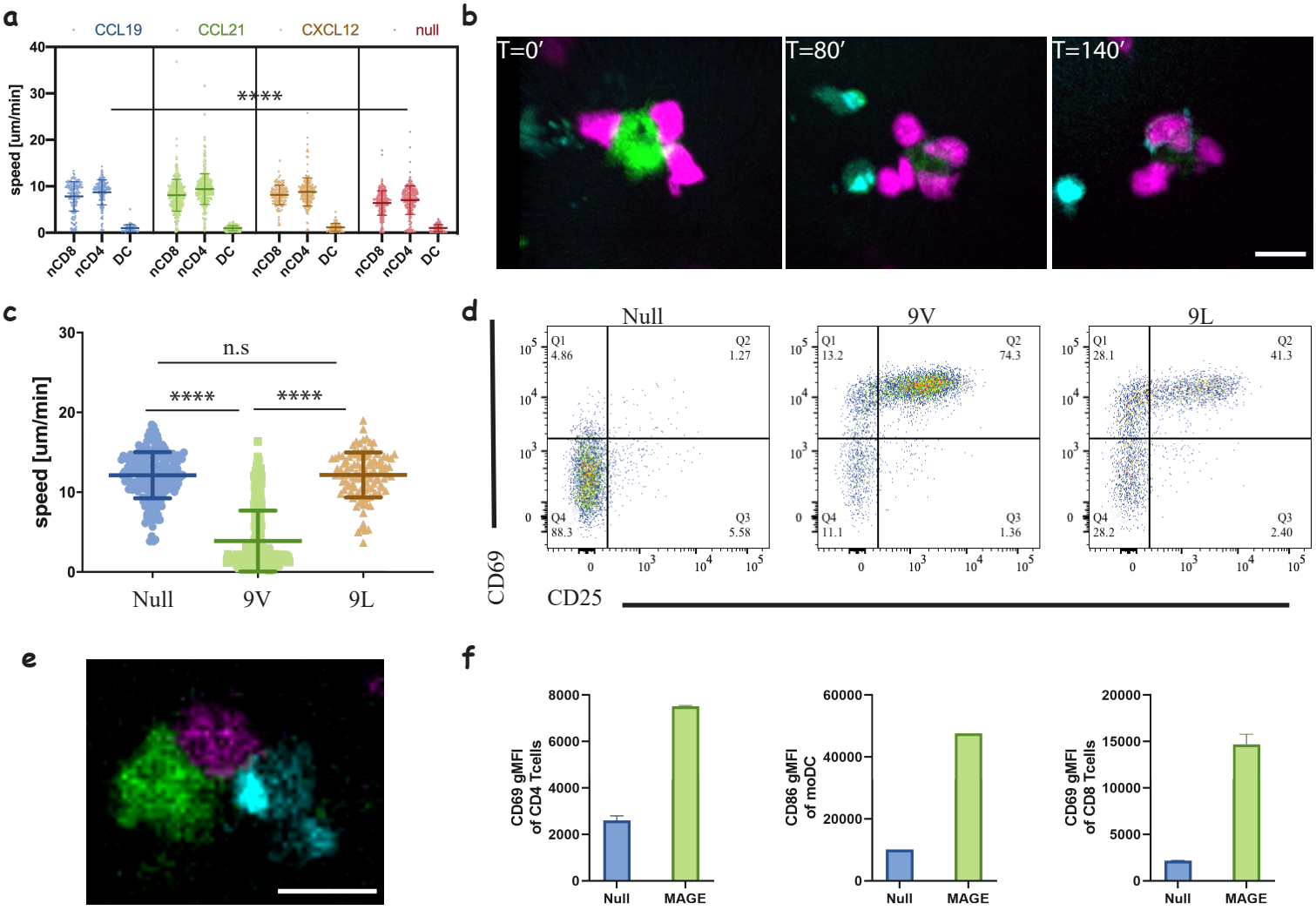

Fig. 2 Abu-Shah et al

bioRxiv preprint doi: https://doi.org/10.1101/587386; this version posted March 24, 2019. The copyright holder for this preprint (which was not certified by peer review) is the author/funder. All rights reserved. No reuse allowed without permission.

Fig.2. Three-Dimensional Culture System to Study Immune Cell Interactions. (a) Motility speeds of naïve CD4 and CD8 T-cells and activated dendritic cells (acDCs) in collagen gels with different chemokines. Note the faster motility of T-cells compared to acDC and equally efficient motility using homeostatic chemokines (CCL19, CCL21 and CXCL12). Representative of 2 independent repeats (Supplementary Video 2, Table 3). (b) Snapshots from a time-lapse movie (Supplementary Video 3) following the interactions of **1G4**-expressing naïve CD8 T-cells (magenta) with antigen loaded acDC (green) in collagen gels containing CXCL12, and the upregulation of CD69 is visible at T=140 min following the accumulation of an anti-CD69 antibody on the surface of the cells (cyan, also in cyan are irrelevant CD4 T-cells). Representative of 3 independent repeats. (c) Speed of **1G4**-expressing naïve CD8 T-cells upon culture in collagen gels containing CXCL12, with acDC either loaded with high affinity (NY-ESO-9V) or low affinity (NY-ESO-9L) peptide or unloaded (null). Note the deceleration of the cells upon engaging with high affinity peptide (3 μm/min compared to 12 μm/min for both null and 9L). Representative of 2 independent repeats. (Supplementary Videos 7-9). (d) The cells from (c) extracted from the collagen gel and run on a flow cytometry to look at CD69 and CD25 as activation markers. Note the good activation despite the absence of T-cell arrest with low affinity peptide (NY-ESO-9L). Representative of more than 3 independent repeats. (e) Co-culture of **1G4**-expressing naïve CD8 T-cells (magenta), **6F9**-expressing naïve CD4 T-cells (cyan) and acDC loaded with 100nM NY-ESO-6T and 10μM MAGE-$A3_{243\text{-}258}$ peptides (green), (Supplementary Video 12), in collagen gels containing CXCL12. (f) Upregulation of CD69 on CD4 (left), and CD8 T-cells (right) and the upregulation of the costimulatory molecule CD86 on acDCs (middle) in the co-culture system from (e) in the presence and absence of MAGE as a stimulus for CD4 T-cells. Representative of at least 3 independent repeats. In all experiments the cell ratio was (5:5:1, CD4: CD8: acDC). Scale bars = 10 μm. (****, $p < 0.0001$, ANOVA)

bioRxiv preprint doi: https://doi.org/10.1101/587386; this version posted March 24, 2019. The copyright holder for this preprint (which was not certified by peer review) is the author/funder. All rights reserved. No reuse allowed without permission.

Supplementary Legend

Supplementary Fig.1. Engineering T-cells with different TCR constructs. (a) Expression of **868** TCR using m RNA electroporation. Also note the improved efficiency after introducing the cysteine modification. Representative of at least 3 independent donors for the **868** and for the Cys modification. Similar results were achieved for **1G4**. (b) Expression of **1G4** in naïve and memory CD8 T-cells. Expression was comparable, although we noticed a slightly lower expression levels in memory T- cells. (c) Histograms of TCR expression following mRNA electroporating of the alpha and beta chain with or without the addition of CD3ζ (right) and quantification of the mean fluorescent intensity (left). Note the increase in efficiency (Representative of N>3). (d) Histograms of TCR expression of three MHC-II restricted TCRs (**6F9**, **R12C9** and **SG6**) (right) and mean quantification of the mean fluorescent intensity (left). Note similar efficiency for **6F9** and **R12C9** compared to significantly lower efficiency of **SG6** (Representative of N>3). (e) Expression of **6F9** TCR by electroporation of naïve (left) or expanded (right) CD4 T-cells (similar results are obtained for **R12C9** and **SG6**).

Supplementary Fig.2. Functional response of mRNA electroporated T-cells. (a) Dose response curve of percent positive (left) and geometric mean (right) of **1G4**-expressing naïve CD8 T-cell upregulating CD69 upon stimulation with peptide loaded acDC, both with low (NY-ESO-4D) and high (NY-ESO-9V) affinity peptides. (b) Dose response curve of naïve CD4s expressing MHC-II restricted TCRs upon stimulation with peptide loaded acDC with either MAGE-A3$_{243-258}$ (for 6F9 and R12C9) or NY-ESO$_{157-180}$ (for SG6). T-cells and DCs are at 1:1 ratio.

Supplementary Fig.3. Interactions of 1G4 expressing naïve CD8 T-cells with pMHC presented on spatially segregated stimulatory spots. (a) The average speed of naïve CD8 T-cells moving on the micropatterned surfaces that have not yet attached to a stimulatory spot (Supplementary Video 1). This is essentially indistinguishable from the speed of untouched naïve CD8 T-cells in an analogous setting [21] (b) The number of cells arresting on spots as a function of time. Gradual accumulation of arrested cells is an indication of efficient search by the T cells and induction of arrest due to TCR-pMHC interactions. The attachment profile is comparable to that of untouched cells engaging with anti-CD3 stimulatory spots [22]. (c) The number of remaining attached cells on stimulatory spots as a function of time after the first 40 minutes of imaging. The linear fit allows the extraction of the life-time of the interactions. Half-life of 4.6 hours compares well with that of untouched cells engaging with anti-CD3 spots [11].

Supplementary Fig.4. Characterising "express" monocyte-derived dendritic cells. (a) The degree of costimulatory molecule upregulation upon maturation for classical DCs and express DCs. (b) Analysis of fold production of cytokines and chemokines released from DC generated in 48 h express procedure comparing original monocytes, the differentiated DCs and matured/activated DCs. An average of three donors where signals bellow 1.5 fold above background were not included. (c) Quantification of the number of NY-ESO-9V peptides loaded on DCs using soluble high affinity TCR (**c113**) and MSEF calibration beads.

bioRxiv preprint doi: https://doi.org/10.1101/587386; this version posted March 24, 2019. The copyright holder for this preprint (which was not certified by peer review) is the author/funder. All rights reserved. No reuse allowed without permission.

Supplementary Fig.5. Motility of T-cells in 3D matrices. (a) Motility of naïve CD8 T-cells cultured in media containing FBS in the presence of different chemokines. Note that in the absence of human serum only the addition of CXCL12 supports cell motility (compared to Fig. 2a). (b) Motility of naïve CD8 T-cells in different matrices, collagen of different origins: human, bovine and non-tryptic bovine, and complex ECM: Matrigel and GelTrex. (**, $p < 0.01$, ANOVA)

Supplementary Fig.6. Calcium Flux upon T-cell/DC conjugate formation. Snapshots from a time-lapse movie (Supplementary Video 4) showing three different **1G4**-expressing CD8 T-cells (magenta), loaded with calcium dye Fluo4-AM (green), interacting with antigen loaded acDCs (100 nM NY-ESO-9V, cyan) in 3D collagen and fluxing calcium (green) upon binding. Note the lower flux in the second and third contacts suggesting lower antigen presentation sequestered by the primary synapse. Scale bar = 10 μm.

Supplementary Fig.7. Different readouts in 3D. (a) Percentage of activated **1G4**- expressing CD8 T-cells as a function of peptide dose similar to Supplementary Fig. 2b, in collagen gels with 5:1 T-cells to DC. (b) Production of interferon gamma from a 24 h co-cultures of **1G4**-expressing CD8 T-cells and peptide loaded acDC with the indicated concentrations of NY-ESO-9V in collagen gels. (c) Proliferation of **1G4**-expressing naïve CD8 T-cells cultured with 100 nM NY-ESO-6T loaded acDC in collagen gels after 72 h, measured by cell trace violet (CTV) dilution. (d) Intracellular staining of activated **1G4**-expressing naïve CD8 T-cells stimulated with high affinity (50 nM, NY-ESO-9V) and low affinity (200 nM, NY-ESO-4D) loaded acDCs at 5:1 ratio, in solution and in collagen gels for comparison. The following markers were tested in the presence and absence of brefeldin A: Granzyme B, LAMP-1 (CD107), IFNγ and TNFα. (e) Activation of **1G4**-expressing naïve CD8 T-cells cultured in collagen gels with either pre-loaded acDCs or acDCs loaded inside the gel (Supplementary Videos 10 & 11 respectively).

Video 1

A time-lapse movie showing gradual increase in the number of arrested cells on stimulatory spots presenting pMHC after some transient interaction events. The image series is a composite overlay of DIC, Interference reflection (IRM) and fluorescence images of the cells and microcontact printed FcIg (green) where cells form an IRM signal indicating spreading and durable interaction with the pMHC presented on stimulatory spots. Scale bar = each circular spot is 10 μm in diameter.

Video 2

3D reconstruction of naïve CD8 (magenta), naïve CD4 (cyan) T-cells, and Dendritic cells (green) moving in 3D collagen gels with RPMI containing human serum and exogenous human CXCL12.

Video 3

3D reconstruction of **1G4**-expressing naïve CD8 T-cells (magenta), interacting with antigen loaded acDCs (100 nM NY-ESO-9V, green) in 3D collagen in the presence of CCL19. Note the transition of cells between different DCs.

bioRxiv preprint doi: https://doi.org/10.1101/587386; this version posted March 24, 2019. The copyright holder for this preprint (which was not certified by peer review) is the author/funder. All rights reserved. No reuse allowed without permission.

Video 4

3D reconstruction of **1G4**-expressing naïve CD8 T-cells (magenta), interacting with antigen loaded acDCs (100 nM NY-ESO-9V, green) in 3D collagen in the presence of CXCL12. Note the intermittent contacts and disengagement of T-cells before re-engaging with a different DCs.

Video 5

3D reconstruction of **1G4**-expressing naïve CD8 T-cells (magenta) interacting with 100 nM NY-ESO-9V loaded acDC (green) in the presence of irrelevant CD4 T-cells (cyan) and a soluble anti-CD69 (cyan). Following conjugate formation, upregulation of CD69 is observed by an accumulation of the antibody (cyan ring) around the CD8 T-cells (magenta).

Video 6

Maximum projection of 3D time-lapse of **1G4**-expressing naïve CD8 T-cells (magenta), loaded with calcium dye Fluo4-AM (green), interacting with antigen loaded acDCs (100 nM NY-ESO-9V, cyan) in 3D collagen and fluxing calcium (green) upon TCR/pMHC engagement.

Video 7

Maximum projection of 3D time-lapse of **1G4**-expressing naïve CD8 T-cells (magenta), interacting with acDCs (green) not loaded with NY-ESO antigenic peptide.

Video 8

Maximum projection of 3D time-lapse of **1G4**-expressing naïve CD8 T-cells (magenta), interacting with antigen loaded acDC (100 nM NY-ESO-9V, green).

Video 9

Maximum projection of 3D time-lapse of **1G4**-expressing naïve CD8 T-cells (magenta), interacting with antigen loaded acDC (100 nM NY-ESO-9L, green).

Video 10

3D reconstruction of **1G4**-expressing naïve CD8 T-cells (magenta), interacting with antigen loaded acDC (100 nM NY-ESO-6T, green).

Video 11

3D reconstruction of **1G4**-expressing naïve CD8 T-cells (magenta), interacting initially unloaded acDCs (green), where the peptide was later added after collagen polymerisation to a final concentration of 100 nM NY-ESO-6T.

Video 12

3D reconstruction of **1G4**-expressing naïve CD8 T-cells (magenta), **6F9**-expressing naïve CD4 T-cells (cyan) interacting with antigen loaded DCs (100 nM NY-ESO-6T and 10 µM MAGE-A3$_{243\text{-}258}$).